

Analytical Description of Polygonal Holes Boring - General Approach

Miodrag Zlokolica* - Maja Čavić - Milan Kostić
Faculty of Technical Sciences, University of Novi Sad, Serbia

Equilateral polygonal holes can be manufactured on conventional machines such as lathes or drills using special tool. Tool has to rotate about its axis while its center simultaneously follows complex planar trajectory. Tool center motion can be achieved in several ways: by guiding tool with template which shape exactly matches the shape of the hole produced, using cam or planetary gears mechanism etc.

To describe accurately polygonal hole boring process it is necessary to determine tool geometry, tool motion as well as realized hole geometry. In order to prescribe optimal boring regime time-history of tool cutting blade tip speed has to be obtained. Holes are, generally, produced with rounded corners so, having in mind further operations with work piece, it is important to know corner radius.

Analytical approach presented in this paper enables easy and efficient forming of the mathematical model describing geometry and kinematics of polygonal hole boring process.

© 2010 Journal of Mechanical Engineering. All rights reserved.

Keywords: polygonal hole, boring, kinematics

0 INTRODUCTION

Polygonal contours of different geometry are widely used in many engineering applications – hexagonal hole in screw head is well known example. In case of the screws, deep extrusion process is used as the only one justified considering number of products, required surface quality and price. However, when there is a need for lesser number of products or they can not be produced using casting of forming, machining technologies has to be applied. Internal surfaces are typically produced using broaching, shaping or EDM procedures while for external ones milling is preferable. Generally, broaching and shaping have problems with accuracy and repeatability of dimensions. EDM gives precise dimensions but it is time-consuming process so, frequently, it is discarded due to high price. On the other side, there exist a lot of machining technologies with main motion based on rotation - motion easiest to obtain. They are rather inexpensive and fast, and among them, most interesting for this problem, is boring. In fact, polygonal holes can be manufactured on conventional machines such as lathes or drills using special tool. It is imperative that tool and hole geometry are compatible, that is to say, hole contour must represent an envelope to consecutive tool positions. Tool has to rotate about its axis while its center simultaneously follows complex planar trajectory. Tool center

motion can be achieved in several ways: by guiding tool with template which shape exactly matches the shape of the hole produced (Watts drilling system [1]), using cam mechanism (Formbore system [2] and [3]) etc. Beside main rotational motion tool has to perform auxiliary linear motion. Watts drill is based on curves of constant width (Roleaux polygons) theory, but it is only applicable on polygonal holes with even number of sides. On the other side when using cams, a different one has to be calculated and applied for each polygonal hole, so it becomes a case study procedure.

In order to prescribe optimal boring regime it is very important to know time-history of tool cutting blade tip speed [4]. Polygonal holes are, generally, produced with rounded corners in order to avoid impact load on the tool, so, having in mind further operations with work piece - assembly for instance, corner radius has to be calculated. Using concept of alternative mechanism [5] and centrodes theory for planar motion [6] those two problems were resolved first graphically for square hole [7]. Analytical approach using centrodes generalized to calculate blade tip velocity and hole corner radius for all types of equilateral polygons was proposed in [8] and [9]. Idea was further developed resulting in general analytical approach which enables easy and efficient forming of the complete mathematical model describing geometry and

*Corr. Author's Address: Faculty of Technical Sciences, Trg Dositeja Obradovića 6, 21000 Novi Sad, Serbia, mzlokolica@uns.ac.rs

kinematics of any equilateral polygonal hole boring process which is presented in this paper.

1 BASIC GEOMETRY OF TOOL AND HOLE

Cross-section of tool for manufacturing equilateral n -sided polygonal hole is an equilateral $n-1$ -sided polygon. During process, trajectories of two tool cutting blade tips coincide with adjacent hole sides, i.e. they actually produce hole sides. Other blades cut rounded corners of the hole.

In Fig. 1 tool and hole geometry parameters relevant for analysis are presented, indexes 1 and 2 refer to tool and hole parameters respectively. Point O is hole center while point C denotes tool center.

Each equilateral polygon can be assembled from triangles with two equal sides. Central angles of these triangles are (n is number of sides of produced polygonal hole):

$$\alpha_1(n) = \frac{2 \cdot \pi}{n-1}, \quad (1)$$

$$\alpha_2(n) = \frac{2 \cdot \pi}{n}. \quad (2)$$

Peripheral angles of tool $\beta_1(n)$ and hole $\beta_2(n)$ are:

$$\beta_1(n) = \frac{n-3}{n-1} \cdot \pi, \quad (3)$$

$$\beta_2(n) = \frac{n-2}{n} \cdot \pi. \quad (4)$$

Mutual position of tool and hole is defined with (valid for $n > 4$):

$$\delta_1(n) = \frac{1}{(n-1) \cdot n} \cdot \pi, \quad (5)$$

$$\delta_2(n) = \frac{(n-2) \cdot (n-3)}{2 \cdot (n-1) \cdot n} \cdot \pi. \quad (6)$$

Tool side dimension can be calculated as:

$$a(n) = A \cdot \cos(\delta_1(n)) + A \cdot \sin(\delta_1(n)) \cdot \tan(\delta_2(n)) \quad (7)$$

if $n > 4$,

$$\text{otherwise } a(4) = A. \quad (8)$$

In case when $n = 4$ tool side dimension can not be calculated accordingly to (7) because tool cutting blade tips will not describe desired hole contour so value defined by (8) is accepted.

Radii of circles circumscribed about tool and hole respectively, $r_1(n)$ and $r_2(n)$, are:

$$r_1(n) = \frac{a(n)}{2 \cdot \sin(\frac{\alpha_1(n)}{2})}, \quad (9)$$

$$r_2(n) = \frac{A}{2 \cdot \sin(\frac{\alpha_2(n)}{2})}. \quad (10)$$

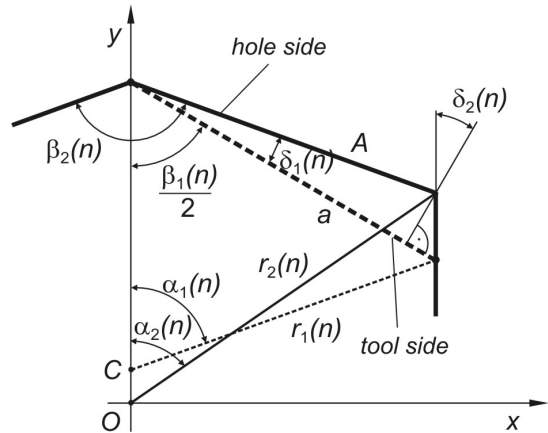


Fig. 1. Tool and hole geometry parameters

2 CHARACTERISTIC POINTS POSITION – FORMING PARAMETRIC EQUATIONS OF MOTION

Characteristic points are: tool center C , tool cutting blade tips and instantaneous velocity pole N . Equations of motion are given with respect to tool rotation angle θ .

2.1 Position of Tool Center - Local Parametric Equation

Origin of fixed coordinate system xOy is positioned in the polygonal hole center O while y axis coincides with axis of symmetry of the hole corner. In case of n -sided polygonal hole this analysis will define only one part of the tool center trajectory that would be the one around the particular corner ($-\theta_g(n) \leq \theta \leq \theta_g(n)$). Tool center position parameters are presented in Fig. 2.

Equations of two adjacent hole sides are:

$$y_1(x, n) = k(n) \cdot x + r_2(n), \quad (11)$$

$$y_2(x, n) = -k(n) \cdot x + r_2(n), \quad (12)$$

where $k(n)$ is given as:

$$k(n) = -\tan\left(\frac{\pi}{2} - \frac{\beta_2(n)}{2}\right). \quad (13)$$

Parametric equation of the cutting tool side is:

$$y_{12}(x, \theta, n) = \tan(\theta) \cdot x + b_{12}(\theta, n), \quad (14)$$

where parameter θ is measured as angle between tool side and x axis.

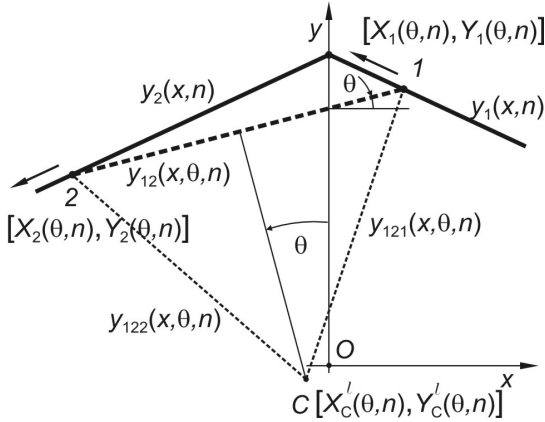


Fig. 2. Tool center position parameters

Coordinates $(X_1(\theta, n), Y_1(\theta, n))$ and $(X_2(\theta, n), Y_2(\theta, n))$ of points 1 and 2 (tool tips), are found as intersection of $(y_{12}(x, \theta, n), y_1(x, n))$ and $(y_{12}(x, \theta, n), y_2(x, n))$ respectively (Fig. 2).

Relation $y_1(x, n) = y_{12}(x, \theta, n)$ is valid for point 1 so it can be written that:

$$X_1(\theta, n) = \frac{r_2(n) - b_{12}(\theta, n)}{\tan(\theta) - k(n)}, \quad (15)$$

$$Y_1(\theta, n) = k(n) \cdot X_1(\theta, n) + r_2(n). \quad (16)$$

In the same way, following expressions can be obtained for point 2:

$$X_2(\theta, n) = \frac{r_2(n) - b_{12}(\theta, n)}{\tan(\theta) + k(n)}, \quad (17)$$

$$Y_2(\theta, n) = -k(n) \cdot X_2(\theta, n) + r_2(n). \quad (18)$$

In those equations $b_{12}(\theta, n)$ represents intersection of line $y_{12}(x, \theta, n)$ and y axis.

It can be calculated using the fact that distance between tool tips i.e. intersection points 1 and 2, of lines $(y_{12}(x, \theta, n), y_1(x, n))$ and $(y_{12}(x, \theta, n), y_2(x, n))$ respectively, always equals $a(n)$. So, if coordinates of point 1 and 2

are $(X_1(\theta, n), Y_1(\theta, n))$ and $(X_2(\theta, n), Y_2(\theta, n))$ it can be written that:

$$(Y_2(\theta, n) - Y_1(\theta, n))^2 + (X_2(\theta, n) - X_1(\theta, n))^2 = a(n)^2. \quad (19)$$

After transformations, expression for $b_{12}(\theta, n)$ is obtained:

$$b_{12}(\theta, n) = r_2(n) - \frac{a(n) \cdot (\tan(\theta)^2 - k(n)^2)}{2 \cdot k(n) \cdot \sqrt{\tan(\theta)^2 + k(n)^2}}. \quad (20)$$

Tool center C is situated at intersection of $y_{121}(x, \theta, n)$ and $y_{122}(x, \theta, n)$ - lines which connect respective tool tip and tool center:

$$y_{121}(x, \theta, n) = a_{121}(\theta, n) \cdot x + b_{121}(\theta, n), \quad (21)$$

$$y_{122}(x, \theta, n) = a_{122}(\theta, n) \cdot x + b_{122}(\theta, n), \quad (22)$$

where $a_{121}(\theta, n)$ and $a_{122}(\theta, n)$ are given as:

$$a_{121}(\theta, n) = \tan\left(\frac{\pi}{2} - \frac{\alpha_1(n)}{2} + \theta\right), \quad (23)$$

$$a_{121}(\theta, n) = \tan\left(\frac{\pi}{2} - \frac{\alpha_1(n)}{2} + \theta\right). \quad (24)$$

Coefficients $b_{121}(\theta, n)$ and $b_{122}(\theta, n)$ are determined using the fact that lines $y_1(x, \theta, n)$ and $y_{121}(x, \theta, n)$ intersects at point 1, while lines $y_2(x, \theta, n)$ and $y_{122}(x, \theta, n)$ intersects at 2.

$$b_{121}(\theta, n) = Y_1(\theta, n) - a_{121}(\theta, n) \cdot X_1(\theta, n), \quad (25)$$

$$b_{122}(\theta, n) = Y_2(\theta, n) - a_{122}(\theta, n) \cdot X_2(\theta, n). \quad (26)$$

Finally, position of tool center C is determined as:

$$X_C^1(\theta, n) = \frac{b_{121}(\theta, n) - b_{122}(\theta, n)}{a_{122}(\theta, n) - a_{121}(\theta, n)}, \quad (27)$$

$$Y_C^1(\theta, n) = a_{121}(\theta, n) \cdot X_C^1(\theta, n) + b_{121}(\theta, n). \quad (28)$$

It is important to emphasize that Eqs. (27) and (28) are valid in $-\theta_g(n) \leq \theta \leq \theta_g(n)$ interval i.e. around axis of symmetry of observed hole corner. Because of that they will be called tool center local equations.

2.2 Position of Fixed Centrode Points – Local Parametric Equations

Fixed centrode presents geometric position of the instantaneous velocity pole (Fig. 3). Since tool cutting blade tips 1 and 2 move along hole sides $y_1(x, n)$ and $y_2(x, n)$, respectively, velocities of 1 and 2 are collinear with $y_1(x, n)$ and $y_2(x, n)$, so intersection of normals to $y_1(x, n)$ and $y_2(x, n)$ at points 1 and 2 represents instantaneous velocity pole N . Equations of lines $y_{1n}(x, \theta, n)$ and $y_{2n}(x, \theta, n)$ are:

$$y_{1n}(x, \theta, n) = a_{1n}(n) \cdot x + b_{1n}(\theta, n), \quad (29)$$

$$y_{2n}(x, \theta, n) = a_{2n}(n) \cdot x + b_{2n}(\theta, n), \quad (30)$$

where:

$$a_{1n}(n) = -\frac{1}{k(n)}, \quad (31)$$

$$a_{2n}(n) = \frac{1}{k(n)}. \quad (32)$$

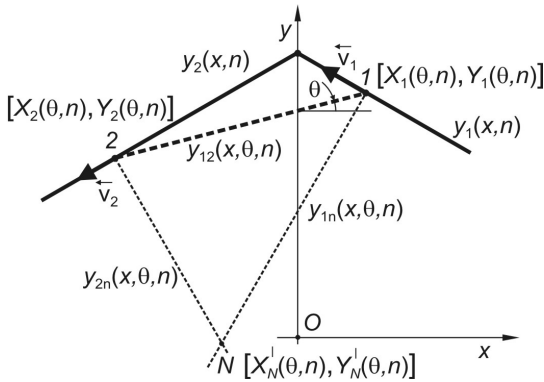


Fig. 3. Instantaneous velocity pole position

Coefficients $b_{1n}(\theta, n)$ and $b_{2n}(\theta, n)$ are determined knowing that lines $y_1(x, n)$ and $y_{1n}(x, \theta, n)$ intersects at 1 ($X_1(\theta, n), Y_1(\theta, n)$), while $y_2(x, n)$ and $y_{2n}(x, \theta, n)$ intersects at 2 ($X_2(\theta, n), Y_2(\theta, n)$).

$$\begin{aligned} b_{1n}(\theta, n) &= \\ &= Y_1(\theta, n) - a_{1n}(\theta, n) \cdot X_1(\theta, n), \end{aligned} \quad (33)$$

$$\begin{aligned} b_{2n}(\theta, n) &= \\ &= Y_2(\theta, n) - a_{2n}(\theta, n) \cdot X_2(\theta, n). \end{aligned} \quad (34)$$

Fixed centrode point (instantaneous velocity pole) N is found as intersection of lines $y_{1n}(x, \theta, n)$ and $y_{2n}(x, \theta, n)$.

Parametric equations defining position of instantaneous velocity pole N are:

$$X_N^l(\theta, n) = \frac{b_{1n}(\theta, n) - b_{2n}(\theta, n)}{a_{2n}(n) - a_{1n}(n)}, \quad (35)$$

$$Y_N^l(\theta, n) = a_{1n}(n) \cdot X_N^l(\theta, n) + b_{1n}(\theta, n). \quad (36)$$

Again, Eqs. (35) and (36) are valid in $-\theta_g(n) \leq \theta \leq \theta_g(n)$ interval i.e. around axis of symmetry of observed hole corner. Because of that they will be called fixed centrode local equations.

2.3 Position of Moving Centrode Points – Local Parametric Equations

Moving centrode is curve rigidly connected to the tool which, while tool moves, rolls without sliding over fixed centrode (Fig. 4). If tool center and fixed centrode points coordinates are known, moving centrode can be easily defined – equation defining position of its points is obtained by expressing fixed centrode points coordinates in local, moving coordinate system x_1Cy_1 . It is rigidly attached to tool, axis y_1 representing axis of symmetry of the tool side and its origin is situated in the tool center C .

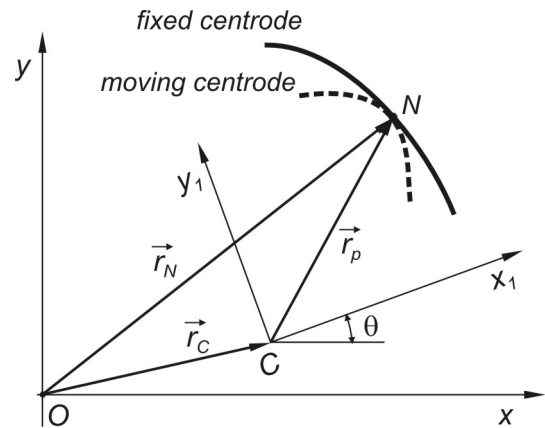


Fig. 4. Fixed and moving centrode

From Fig. 4 it can be seen:

$$\vec{r}_N = \vec{r}_C + \vec{r}_p. \quad (37)$$

Using matrix transformation between x_1Cy_1 and xOy following relation can be written:

$$\begin{bmatrix} X_N^1(\theta, n) \\ Y_N^1(\theta, n) \\ 0 \end{bmatrix} = \begin{bmatrix} \cos(\theta) & -\sin(\theta) & X_C^1(\theta, n) \\ \sin(\theta) & \cos(\theta) & Y_C^1(\theta, n) \\ 0 & 0 & 0 \end{bmatrix} \cdot \begin{bmatrix} X_P^1(\theta, n) \\ Y_P^1(\theta, n) \\ 1 \end{bmatrix}, \quad (38)$$

which, after some transformations, gives local equations of moving centre:

$$\begin{bmatrix} X_P^1(\theta, n) \\ Y_P^1(\theta, n) \\ 0 \end{bmatrix} = \begin{bmatrix} \cos(\theta) & \sin(\theta) & -X_C^1(\theta, n) \cdot \cos(\theta) - Y_C^1(\theta, n) \cdot \sin(\theta) \\ -\sin(\theta) & \cos(\theta) & X_C^1(\theta, n) \cdot \sin(\theta) - Y_C^1(\theta, n) \cdot \cos(\theta) \\ 0 & 0 & 0 \end{bmatrix} \cdot \begin{bmatrix} X_N^1(\theta, n) \\ Y_N^1(\theta, n) \\ 1 \end{bmatrix}. \quad (39)$$

2.4 Position of Fixed Centrode Points, Tool Center and Moving Centrode Points – Global Parametric Equations

First, global parametric equations for fixed centrode points will be determined. Locally, fixed centrode is defined with $(X_N^1(\theta, n), Y_N^1(\theta, n))$, where angle θ is parameter. Manufactured polygonal hole represents centrally symmetrical curve which implies central symmetry of fixed centrode. Furthermore, that suggests transition from Descartes to polar coordinates:

$$r_N^1(\theta, n) = \sqrt{X_N^{12}(\theta, n) + Y_N^{12}(\theta, n)}, \quad (40)$$

$$\phi_N^1(\theta, n) = \arctan\left(\frac{X_N^1(\theta, n)}{Y_N^1(\theta, n)}\right). \quad (41)$$

As problem geometry is same around axis of symmetry of each hole corner it is obvious that fixed centrode has to be periodical curve with period:

$$\phi_{NT}(n) = \alpha_2(n). \quad (42)$$

Eqs. (40) and (41) are highly nonlinear with respect to parameter, so it is not possible to obtain analytical expression $r_N^1 = r_N^1(\phi_N^1)$. On

the other hand, period θ_g of the parameter can be calculated using relationship:

$$\phi_N^1(\theta_g, n) = \phi_{NT}(n). \quad (43)$$

In this way, an interval $(-\theta_g \leq \theta \leq \theta_g)$ around one axis of symmetry (one hole corner) in which local equations are valid can be determined. Polar radius of global curve is periodical function of polar angle ϕ_N^1 with period $\phi_{NT}(n) = \alpha_2(n)$ but it is also periodical function of θ , with period $2\theta_g$.

In order to calculate global radius $r_N = r_N(\theta, n)$ of fixed centrode expansion of (41) to Fourier series will be used on interval $-\frac{\alpha_2(n)}{2} \leq \phi_N^1(n) < \frac{\alpha_2(n)}{2}$.

Using property of Fourier series which says that if a function is expanded on interval, than Fourier series not only represents function approximation on that interval but it will also be its periodical continuation, global radius of fixed centrode can be calculated for whole period $\phi_N(\theta, n) \in (0 \dots 2\pi)$.

As said before geometry of polygonal hole is symmetrical with respect to y axis (Figs. 2 and 3). Since geometry of the fixed centrode is determined by the geometry of the polygonal hole, centrode itself has to be symmetrical with respect to y axis. This means that local radius (41) has to be even function i.e.:

$$r_N^1(\phi_N^1) = r_N^1(-\phi_N^1), \quad (44)$$

$$\text{or } r_N^1(\theta, n) = r_N^1(-\theta, n). \quad (45)$$

Because of that, expansion to Fourier series can be simplified and global radius of fixed centrode can be finally expressed as:

$$r_N(\theta, n) = \frac{Af_0(n)}{2} + \sum_{i=1}^{\infty} Af_i(n) \cdot \cos\left(\frac{i \cdot \pi}{\phi_{PNT}(n)} \cdot \theta\right), \quad (46)$$

where $Af_i(n)$ are Fourier coefficients which are determined as:

$$Af_i(n) = \frac{2}{\phi_{NT}(n)} \cdot \int_{-\frac{\phi_{NT}(n)}{2}}^{\frac{\phi_{NT}(n)}{2}} r_N^1(\theta, n) \cdot \cos\left(\frac{i \cdot \pi}{\phi_{NT}} \cdot \theta\right) d\theta. \quad (47)$$

Polar angle function angle is also periodical function with period $\phi_{NT}(n)$ (parameter period is $2 \cdot \theta_g$). In order to define global curve of the fixed centrod polar angle has to fill complete interval $\varphi_N(\theta, n) \in (0 \dots 2\pi)$. From Fig. 5 it is obvious that global function of the polar angle can be obtained by continuous supervening of polar angle local functions $\phi_N^1(\theta, n)$ until $\phi_N(\theta, n)$ reaches 2π . So, as in interval $(0 \dots 2\pi)$ there are n periods $(n \cdot \varphi_{NT}(n) = 2\pi)$, local function $\phi_N^1(\theta, n)$ has to be added n times in order to form $\varphi_N(\theta, n)$. While parameter θ changes in interval $0 \leq \theta < 2 \cdot n \cdot \theta_g$ polar angle describes whole fixed centrod i.e. $\varphi_N(\theta, n) \in (0 \dots 2\pi)$.

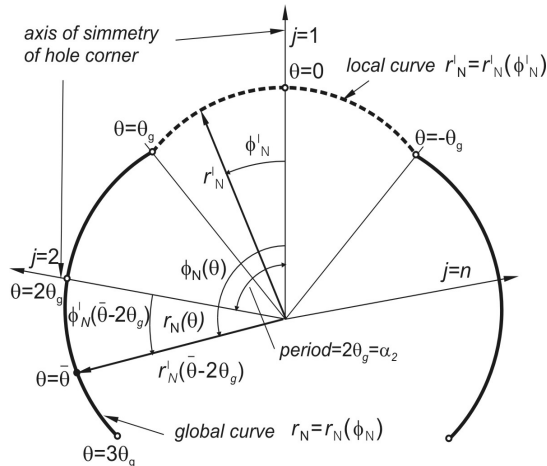


Fig. 5. Fixed centrod – global curve

Index j is introduced, defining an interval in which instantaneous value of parameter θ is situated:

$$j = \text{whole part of } \left(\frac{\theta}{2 \cdot \theta_g} \right). \quad (48)$$

Global function of the polar angle can now be written as:

$$\begin{aligned} \phi_N(\theta, n) &= \\ &= \phi_N(\theta - 2 \cdot j \cdot \theta_g, n) + j \cdot \phi_{NT}(n). \end{aligned} \quad (49)$$

Obtained curve: $\phi_N(\theta, n)$, $r_N(\theta, n)$ (Eqs. (46) and (49)) represents fixed centrod global curve ($\varphi_N(\theta, n) \in (0 \dots 2\pi)$ while $0 \leq \theta \leq 2 \cdot n \cdot \theta_g$) (Fig. 5).

Same procedure can be applied in order to form tool center global curve $\phi_C(\theta, n)$, $r_C(\theta, n)$.

Some interesting conclusions have been obtained while performing the procedure. Namely, after forming and analyzing global equation for radius of tool center trajectory $r_C(\theta, n)$ it was concluded that trajectory has nearly circular shape. Eccentricity of trajectory, is introduced as:

$$e(n) = \frac{\max(r_C(\theta, n))}{\min(r_C(\theta, n))}. \quad (50)$$

It resumes values significantly close to 1 for all cases of n .

Also, after analysis of polar angle global function $\phi_C(\theta, n)$ (Fig. 6) it has been concluded that it behaves close to function:

$$\phi_C(\theta, n) = -(n-1) \cdot \theta. \quad (51)$$

Differentiation of (51) gives relationship between angular velocities in the following form:

$$\dot{\phi}_C(\theta, n) = -(n-1) \cdot \dot{\theta}. \quad (52)$$

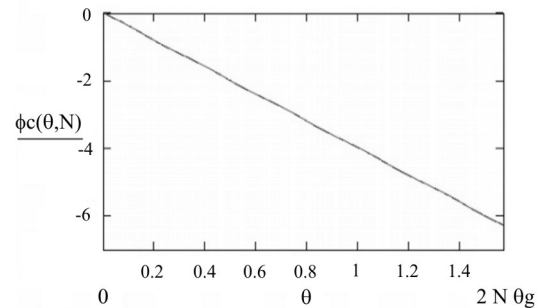


Fig. 6. Function $\phi_C(\theta, n)$ with respect to θ (case $n = 5$)

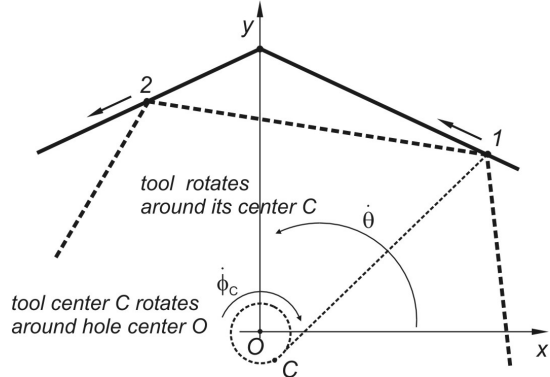


Fig. 7. Tool motion

This means that tool motion (Fig. 7.) can be realized as superposition of two rotations: tool has to rotate around its longitudinal axis with angular velocity $\dot{\theta}$ and, at the same time, to rotate around hole centre O with angular velocity $\dot{\phi}_C$, radius of rotation is equal to average $(r_C(\theta, n))$. Such motion can be easily realized using planetary gear mechanism.

Moving centrode global curve $\phi_p(\theta, n)$ $r_p(\theta, n)$ can be defined following the same procedure. It is also centrally symmetrical and periodical curve, its period depending on its shape. Since tool geometry defines shape of moving centrode period of global polar angle $\phi_p(\theta, n)$ will be:

$$\phi_{PT}(n) = \frac{2 \cdot \pi}{n-1} = \alpha_1(n) . \quad (53)$$

Obtained curve gives coordinates in moving coordinate system $x_l C y_l$. Its origin is positioned at the tool center $X_C(\theta, n)$, $Y_C(\theta, n)$, while axis x_l forms angle θ with axis x of fixed coordinate system $x O y$. Now, moving centrode can be expressed in fixed coordinate system using following matrix transformation:

$$\begin{bmatrix} X_p^f(\theta, n) \\ Y_p^f(\theta, n) \\ 0 \end{bmatrix} = \begin{bmatrix} \cos(\theta) & -\sin(\theta) & X_C(\theta, n) \\ \sin(\theta) & \cos(\theta) & Y_C(\theta, n) \\ 0 & 0 & 0 \end{bmatrix} \cdot \begin{bmatrix} X_p(\theta, n) \\ Y_p(\theta, n) \\ 1 \end{bmatrix} . \quad (54)$$

where $X_p(\theta, n)$ and $Y_p(\theta, n)$ are Descartes coordinates of moving centrode in moving coordinate system.

2.5 Position of Tool Cutting Blades Tips

In case of manufacturing n -sided equilateral polygonal hole, tool has to have shape of $n-1$ -sided equilateral polygon, two of its corners being in contact with hole sides.

Parameter m which defines tool cutting blades tip index is introduced. With known global position of tool center $X_C(\theta, n)$, $Y_C(\theta, n)$, distance $r_1(n)$ between tool center and tool tip as well as angle $\gamma(\theta, n, m)$, it is easy to calculate position of

all tool cutting blades tips $m = 1, 2, 3, \dots, n-1$ (Fig. 8):

$$\begin{bmatrix} X_m(\theta, n) \\ Y_m(\theta, n) \end{bmatrix} = \begin{bmatrix} X_C(\theta, n) \\ Y_C(\theta, n) \end{bmatrix} + \begin{bmatrix} -\sin(\gamma(\theta, n, m)) \\ \cos(\gamma(\theta, n, m)) \end{bmatrix} \cdot r_1(n) . \quad (55)$$

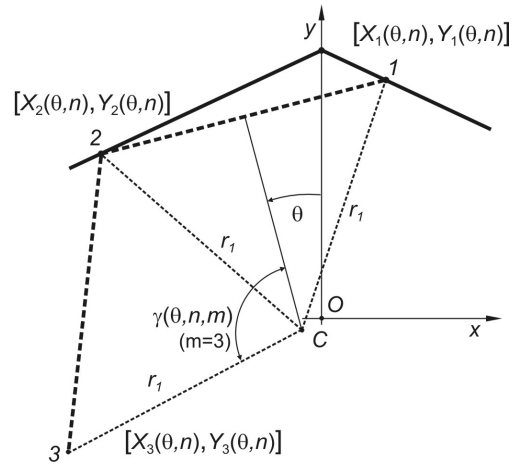


Fig. 8. Position of tool cutting blades tips

Tool tips $m = 1, 2$ are situated on hole sides. Angle $\gamma(\theta, n, m)$, is calculated as:

$$\gamma(\theta, n, m) = \frac{\alpha_1(n)}{2} + \alpha_1(n) \cdot (m-2) + \theta . \quad (56)$$

Since global coordinates of tool center were used in Eq. (55), obtained $X_m(\theta, n, m)$ and $Y_m(\theta, n, m)$ represent global coordinates of m th tool tip.

After forming trajectory of each tool tip ($m = 1, 2, \dots, n-1$) for one period ($\theta = 0 \dots 2 \cdot n \cdot \theta_g$) they are combined thus forming closed curve which represents contour of real manufactured hole (Fig. 9).

2.6 Radius of Curvature of Tool Cutting Blades Tip Trajectory

In general, if the moving point trajectory is defined by $\vec{r}(s)$, (s is the parameter) than its radius of curvature is defined as:

$$\rho(s) = \frac{|\dot{\vec{r}}(s)|^3}{|\dot{\vec{r}}(s) \times \ddot{\vec{r}}(s)|} . \quad (57)$$

In this case tool tip coordinates are $X_m(\theta, n, m)$, $Y_m(\theta, n, m)$, so its position vector in xOy is given as:

$$\vec{r}_m(\theta, n, m) = X_m(\theta, n, m) \cdot \vec{i} + Y_m(\theta, n, m) \cdot \vec{j} \quad (58)$$

Radius of curvature is then (acc. to Eq. (57)):

$$\rho(\theta, n, m) = \frac{|\dot{\vec{r}}_m(\theta, n, m)|^3}{|\dot{\vec{r}}_m(\theta, n, m) \times \ddot{\vec{r}}_m(\theta, n, m)|} \quad (59)$$

or, after differentiation with respect to θ :

$$\rho(\theta, n, m) = \frac{|\sqrt{\dot{X}_m(\theta, n, m)^2 + \dot{Y}_m(\theta, n, m)^2}|^3}{|\dot{X}_m(\theta, n, m) \cdot \ddot{Y}_m(\theta, n, m) - \ddot{X}_m(\theta, n, m) \cdot \dot{Y}_m(\theta, n, m)|} \quad (60)$$

When tool tip enters hole corner radius of curvature decreases, so it assumes its minimal value ρ_{\min} at positions defined by :

$$\theta_{\min} = 0, 2 \cdot \theta g, 4 \cdot \theta g \dots 2 \cdot n \cdot \theta g \quad (61)$$

Those positions are determined by parameter period $2 \cdot \theta g$ (Fig. 5).

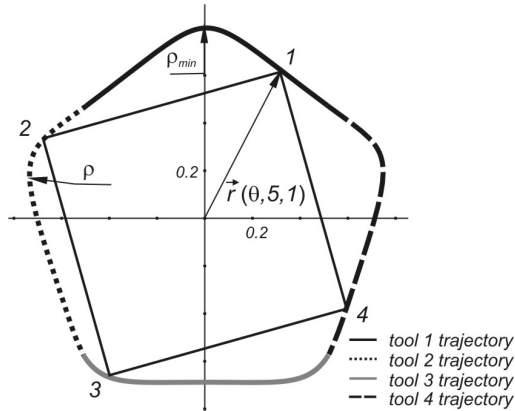


Fig. 9. Real contour of the manufactured polygonal hole (case $n = 5$)

Corner radius ρ_{\min} , minimal corner radius ρ_{\min} , tool tips 1, 2, 3 and 4 position vector and trajectories for one period, as well as complete hole contour for case $n = 5$, are presented in Fig. 9.

2.7 Tool Cutting Blades Tip Velocity

With position of tool tip known it is easy to calculate its velocity vector:

$$\vec{v}_m(\theta, n, m) = \dot{\vec{r}}_m(\theta, n, m) = \dot{X}_m(\theta, n, m) \cdot \vec{i} + \dot{Y}_m(\theta, n, m) \cdot \vec{j} \quad (62)$$

Absolute value of velocity is obtained as:

$$v_m(\theta, n, m) = \sqrt{\dot{X}_m(\theta, n, m)^2 + \dot{Y}_m(\theta, n, m)^2} \quad (63)$$

3 EXAMPLE – PENTAGONAL HOLE BORING

Hole profile is equilateral pentagon so tool will have square shape. Necessary geometrical parameters, according to Eqs. (1) to (9) have been calculated:

- tool and hole central angles:
 $\alpha_1(5) = 90^\circ$, $\alpha_2(5) = 72^\circ$,
- tool and hole peripheral angles:
 $\beta_1(5) = 90^\circ$, $\beta_2(5) = 108^\circ$,
- angles determining mutual position of tool and hole: $\delta_1(5) = 9^\circ$, $\delta_2(5) = 27^\circ$,
- dimension of tool side: It was adopted that $A = 1$ cm, so $a(5) = 1.05$ cm,
- radii of circles circumscribed about tool and hole: $r_1(5) = 0.741$ cm, $r_2(5) = 0.851$ cm.

Using procedure derived in Section 2 graphs presenting position of tool center (Fig. 10), fixed centre (Fig. 11), moving centre (Fig. 12), real contour of the manufactured polygonal hole (Fig. 9) and tool cutting blade tip velocity (Fig. 13) are obtained.

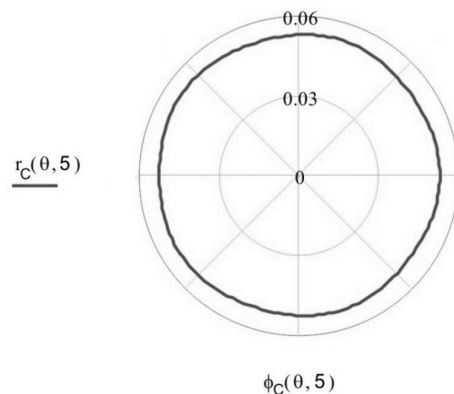


Fig. 10. Position of tool center ($\varphi_c(\theta, 5)$, $r_c(\theta, 5)$)

Change of tool cutting blade tip velocity with respect to θ is presented in Fig. 13.

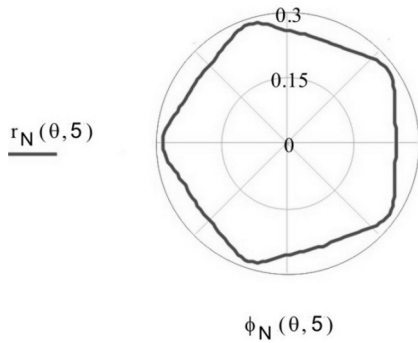


Fig. 11. Fixed centrode ($\varphi_N(\theta, 5)$, $r_N(\theta, 5)$)

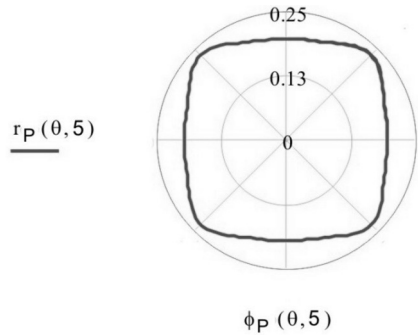


Fig. 12. Moving centrode ($\varphi_P(\theta, 5)$, $r_P(\theta, 5)$)

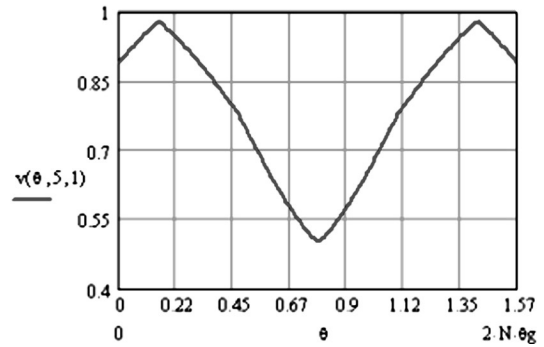


Fig. 13. Tool cutting blade tip velocity

Minimal radius of curvature appears at the hole corners, for pentagonal hole $\rho_{\min} = 0.17 \text{ cm}$.

One period of hole boring process (corresponding to one turn of centrodes) is presented in Fig. 14. Moving centrode rolls over fixed one thus realizing tool motion. During the motion tool center C describes nearly circular curve K .

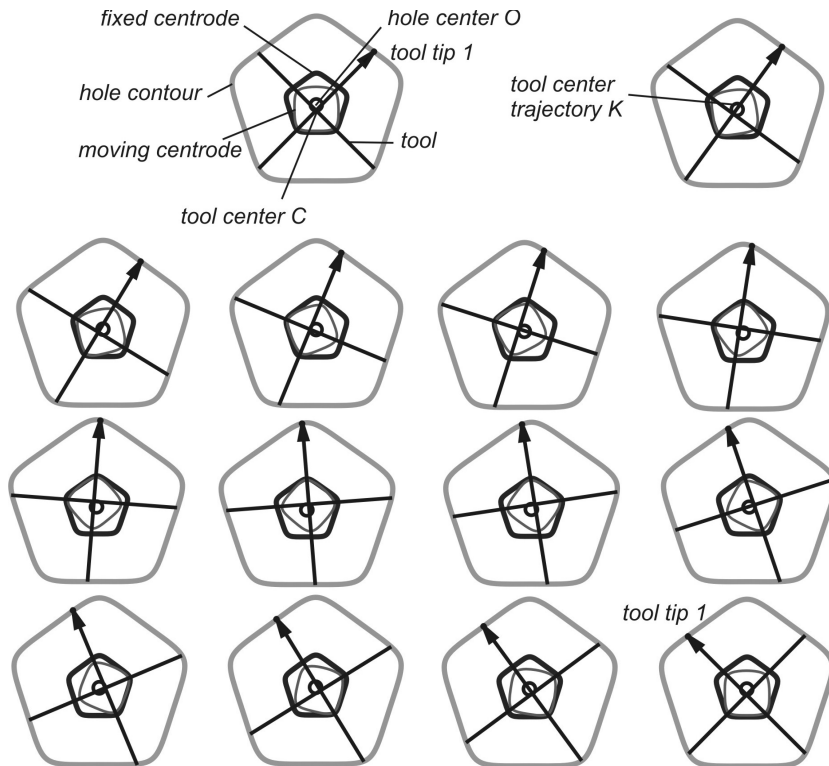


Fig. 14. Pentagonal hole boring process

In Working model 2D software planetary gear mechanism that realizes desired motion i.e. moves tool so it cuts desired equilateral pentagonal hole has been modeled and tool motion was simulated (Fig. 15).

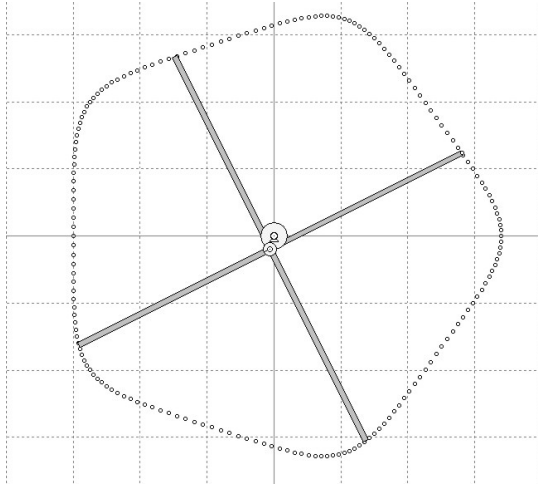


Fig. 15. Simulation of tool motion

4 CONCLUSION

Using proposed analytical approach it is possible to analyze geometry and kinematics of tool in the process of boring equilateral polygonal hole.

Cross-section of tool for manufacturing equilateral n -sided polygonal hole is an equilateral $n-1$ -sided polygon where cutting blades are positioned in respective tool tips and are always in contact with hole sides. Such geometry implies that hole corner will be cut with respective radius and the difference (distance between tool tip and hole corner) measures less than 5% of hole side A . Value of ρ_{\min} rises with A and, even more, with n (number of hole sides). For $n > 10$, a radius becomes significant, but having in mind that such a hole, even with precise geometry, slightly differs from a circle, it is not widely used and this fact does not limitate the usefulness of the method. Though existence of the radii is preferable because of better dynamic regime of cutting, in some cases it is necessary to cut hole with precise geometry. This can be done by reshaping the tool and making its center to follow an appropriate trajectory, which, in practice, leads to application of single cutting tip tool with cam mechanism. As for shape of hole sides, taking enough members in Eq. (46) ensures satisfactory precision.

Presented approach as well as the method used to solve the problem is general – applicable to all equilateral polygons, not only to 4, 6 and 8-sided as methods based on curves of constant width. Even though the holes are cut with radius in corners, the fact that multiple tool tips are in contact with hole sides ensures good dynamics of boring regime (no impact in sharp corners, cutting force is distributed to more cutting blades thus diminishing stress to the tool). Also, a simple practical solution – planetary gear mechanism which can realize desired motion is proposed (no need for complex tool center trajectory realization – cams or robot guidance (EDM)).

5 REFERENCES

- [1] Polygon Hole Drill. Retrived on 1.2.2009, from <http://www.inigerspin.co.uk/polygon.htm>.
- [2] Koepfer, C. (1995). *Boring non round holes*, Modern Machine shop. Retrived on 1.02.2009 from <http://www.mmmsonline.com>.
- [3] *Form drilling or turning device* (1996). US patent, Patent Number 5,542,324.
- [4] Bajić, D., Lela, B., Cukor, G. (2008). Examination and modeling of the influence of cutting parameters on the cutting force and the surface roughness in longitudinal turning. *Strojniški vestnik - Journal of Mechanical Engineering*, vol. 54, no. 5, p. 322-333.
- [5] Norton, R.L. (1992). *Design of Machinery*, McGraw-Hill, Inc., New York.
- [6] Erdman, A.G., Sandor, G.N. (1984). *Advance mechanism design, analysis and synthesis*, vol. 2. Prentice Hall, Inc., New Jersey.
- [7] Zlokolica, M. (1975). Kinematics of tools for polygonal drilling. *Journal of Technique, Mechanical section*, vol. 24, no. 6, p. 15-18.
- [8] Zlokolica, M., Čavić, M., Kostić, M. (1999). Centroides in the process of kinematic description of the tools for the polygonal holes production. *Proceedings of 1st International Conference The Coating in Manufacturing Engineering*, p. 663-671, Thessaloniki, October 14.-15.
- [9] Zlokolica, M., Sovilj, B., Čavić, M., Kostić, M. (2000). About the blade cutting speed of the tools for boring polygonal holes. *Proceedings of 10th International Conference on Tools*, p. 277-281, Miskolc, September 6.-8.